

J.O. Bustamante · E.R.F. Michelette · J.P. Geibel  
David A. Dean · J.A. Hanover · T.J. McDonnell

## Calcium, ATP and nuclear pore channel gating

Received: 8 September 1999 / Received after revision: 4 October 1999 / Accepted: 5 October 1999 / Published online: 23 November 1999

**Abstract** Nuclear envelope (NE) cisternal  $\text{Ca}^{2+}$  and cytosolic ATP are required for nuclear-pore-complex- (NPC-) mediated transport of DNAs, RNAs, transcription factors and other large molecules. Isolated cardiomyocyte nuclei, capable of macromolecular transport (MMT), have intrinsic NPC ion channel behavior. The large ion conductance ( $\gamma$ ) activity of the NPC channel (NPCC) is blocked by the NPC monoclonal antibody mAb414, known to block MMT, and is also silenced during periods of MMT. In cardiomyocytes, neither cytosolic  $\text{Ca}^{2+}$  nor ATP alone directly affects NPCC gating. To test the role of  $\text{Ca}^{2+}$  and ATP in NPCC activity, we car-

ried out the present patch-clamp study with the pipette attached to the outer NE membrane of nuclei isolated from cultured Dunning G prostate cancer cells. Our investigations demonstrate that in these isolated nuclei neither cytosolic  $\text{Ca}^{2+}$  nor ATP alone directly affects NPCC gating. However, when simultaneously applied to the bath and pipette, they transiently silence NPCC activity through stimulation of MMT by raising the  $\text{Ca}^{2+}$  concentration in the NE cisterna ( $[\text{Ca}^{2+}]_{\text{NE}}$ ). Our fluorescence microscopy observations with nuclear-targeted macromolecular fluorochromes (B-phycoerythrin and plasmid for the enhanced green fluorescence protein EGFP, pEGFP-C1) and with FITC-labeled RNA support the view that channel silence accompanies MMT. Repeated  $\text{Ca}^{2+}$  loading of the NE with  $\text{Ca}^{2+}$  and ATP, after unloading with 1–5  $\mu\text{M}$  inositol 1,4,5-trisphosphate ( $\text{IP}_3$ ), thapsigargin (TSG) or 5 mM BAPTA or EGTA, failed to affect channel gating. This result indicates that other factors are involved in this phenomenon and that they are exhausted during the first cycle of NE  $\text{Ca}^{2+}$  loading/unloading – in agreement with current theories of NPC-mediated MMT. The results explain how  $\text{Ca}^{2+}$  and  $\text{IP}_3$  waves may convert the NE into an effective  $\text{Ca}^{2+}$  barrier and, consequently, affect the regulation of gene activity and expression through their feedback on MMT and NPCC gating. Thus,  $[\text{Ca}^{2+}]_{\text{NE}}$  regulation by intracellular messengers is an effective mechanism for synchronizing gene activity and expression to the cellular rhythm.

**Key words** ATP · Calcium · Calcium ion channels · Cancer cells · Dunning G prostate · Gene activity · Gene expression · Gene regulation · Nuclear · Nuclear envelope · Nuclear pores

J.O. Bustamante · E.R.F. Michelette  
The Nuclear Physiology Laboratory, Universidade Tiradentes,  
Aracaju, Sergipe 49030–270, Brazil

J.O. Bustamante  
Dept. Medicine, Yale University School of Medicine,  
New Haven, CT 06520, USA

J.O. Bustamante · J.P. Geibel  
Dept. Surgery, Yale University School of Medicine,  
New Haven, CT 06520, USA

J.P. Geibel  
Dept. Cellular and Molecular Physiology,  
Yale University School of Medicine,  
New Haven, CT 06520, USA

D.A. Dean  
Dept. Microbiology and Immunology,  
University of South Alabama College of Medicine,  
Mobile, AL 36688–0002, USA

J.A. Hanover  
Lab. Cell Biochemistry, NIDDK, National Institutes of Health,  
Bethesda, MD 20892–0850, USA

T.J. McDonnell  
Dept. Molecular Pathology, The University of Texas,  
M.D. Anderson Cancer Center, Houston, TX 77030, USA

J.O. Bustamante (✉)  
Professor Titular, Director, The Nuclear Physiology Laboratory,  
Universidade Tiradentes, Rua B-508, Praia Aruana,  
Aracaju, Sergipe 49037–610, Brazil  
e-mail: omar@unitnet.com.br  
Tel.: +55-79-9884320, Fax: +55-79-2433661

### Introduction

DNAs, RNAs, transcription factors and other large molecules essential to the control of gene activity and expression cross the nuclear envelope (NE) exclusively through the nuclear pore complex (NPC). The NPC, the only di-

rect pathway connecting the nucleus and cytoplasm, is a large supramolecular structure of about 126 MDa [1]. Under electron and atomic force microscopy (EM and AFM, respectively), most NPCs display a central plug when the specimen is prepared under conditions unfavorable to macromolecular transport (MMT); whereas the NPCs are unplugged when specimens are prepared under MMT-favorable conditions ([1, 2] – reviewed in [3]). Studies with AFM and field-emission scanning electron microscopy (FESEM), two surface/topological techniques (see [2, 3]), demonstrated that, in isolated nuclei, the detection of the putative NPC plug depends on the  $\text{Ca}^{2+}$  concentration in the NE ( $[\text{Ca}^{2+}]_{\text{NE}}$ ) and, therefore, that the appearance of the plug is connected to the translocation of particles of relative mass,  $M_r$ , greater than 500 Da ([4, 5, 6], reviewed in [7]). NPCs may be plugged by reducing  $[\text{Ca}^{2+}]_{\text{NE}}$ , which explains the fluorescence and luminescence microscopy observations that, under certain conditions, the NE is capable of monoatomic ion-barrier behavior (e.g., [8, 9] – reviewed in [10, 11, 12]). Furthermore, small dextran molecules (e.g., <10 kDa) placed outside the nucleus translocate into the nuclear interior and not into the NE cisterna [13, 14, 15], demonstrating that only the NPCCs, and not channels at either of the two NE membranes, provide an electrical and chemical short-circuit between the pipette and bath electrodes in nucleus-attached patch-clamp preparations. Recent independent patch-clamp and fluorescence microscopy studies confirm this view [16, 17]. That is, nuclei isolated at our laboratory (e.g., [18, 19]) and elsewhere (e.g., [15]) show that the NE cisterna is isolated from the extra- and intra-nuclear compartments. AFM has also been used to show that extranuclear  $\text{Ca}^{2+}$  and ATP can induce changes in NPC shape ([20] and [21], respectively). To date, no-one has shown that NPC channels (NPCCs) are permanently closed to monoatomic ion flow. However, in contrast, it has been shown that, at the macroscopic level, both monoatomic ions and small molecules enter the nucleus under the most unphysiological conditions (e.g., [14, 15]). We showed, in a series of reports combining patch-clamp with laser scanning confocal microscopy (and supported with EM and AFM), that the NPC of isolated cardiomyocyte nuclei has an intrinsic ion channel behavior that can be transiently and reversibly silenced (i.e., the measured ion current is zeroed) by transcription factors and other nuclear macromolecules in a fashion that suggests transient plugging of the NPCC [18, 22, 23]. Isolated cardiomyocyte nuclei display all known properties of the NPC-mediated transport of monoatomic ions, small- and medium-sized molecules as well as macromolecules [18], and their distinct large-ion-conductance ( $\gamma$ ) channel activity is blocked by the NPC monoclonal antibody mAb414, known to block MMT (cf. [18]). These investigations, and those previously published by us and others, led us to conclude that the NPCC is responsible for such channel activity and that macromolecules moving along the NPCC plug it during their translocation ([18, 24]; see [25]). The observation that macromolecules silence other

large- $\gamma$  ion channels by plugging them is not new. Mitochondrial peptides and proteins silence the mitochondrial PSC, VDAC and MCC channels (e.g., [26, 27, 28, 29, 30, 31]). Mazzanti and coworkers reported that, in situ nuclei from *Xenopus laevis* oocytes, cytosolic  $\text{Ca}^{2+}$  and ATP affect NE ion permeability and channel conductance [32, 33]. However, our studies with nuclei isolated from adult cardiac myocytes failed to show a direct action of either agent alone on single NPCC gating [11, 19]. To determine whether our apparent discrepant observations of NPCC channel gating result from differences in the starting/control  $[\text{Ca}^{2+}]_{\text{NE}}$  levels (related to specimen preparation) and the accompanying differences of NPC-mediated MMT, we designed the present nucleus-attached patch-clamp studies with cultured Dunning G prostate cancer cells. Our investigations indicate that although  $\text{Ca}^{2+}$  and ATP do not directly affect the large- $\gamma$  NPCC activity when acting independently, they do modify NPCC gating via their concerted indirect action on  $[\text{Ca}^{2+}]_{\text{NE}}$  which is a requirement for MMT. Translocating macromolecules, in turn, counter ion flow along the NPCC, resulting in the transient silencing of NPCC activity. MMT transiently converts the NE into an effective  $\text{Ca}^{2+}$  barrier which, in turn, modulates gene regulation by transcription factor entry and expression via DNA entry into and RNA exit from the nucleus. Thus stimuli causing  $\text{Ca}^{2+}$  depletion from the NE appear to be a mechanism by which the cells synchronize their gene activity and expression to their functional rhythm. Our observations of events in isolated nuclei may be relevant to in situ conditions, as is indicated by the recent demonstration of NE dissociation from the endoplasmic reticulum when cytosolic  $\text{Ca}^{2+}$  is raised [34].

---

## Materials and methods

### Nuclei isolation

Dunning G prostate cancer cells were cultured according to standard procedures. Confluent cells (about  $10^6$ – $10^7$  cells) were scraped in their medium with a rubber policeman from their 75-cm<sup>2</sup> culture flask. The cell suspension in its culture medium (RPMI-1640+10% fetal bovine serum, Sigma, St. Louis, Mo., USA) was centrifuged for 3 min at 2000 rpm, 4°C (Sorvall RC-5C Plus, Dupont, Wilmington, Det., USA). The cell pellet was then washed with 4°C high-K-EGTA solution (mM: 135 KCl, 5 EGTA, 5  $\text{MgCl}_2$ , 10 HEPES, and 15 KOH, pH 7.2). The pellet in 10 ml of this solution was placed in a Dounce manual tissue grinder (Wheaton-33 low extractable borosilicate glass; Wheaton, Millville, N.J., USA). Nuclei were released by four to six strokes with the loose-fitting pestle of the tissue grinder. Nuclei were purified in Percoll gradient as we previously described for cardiac myocytes [35].

### Solutions

Cytosolic  $[\text{K}^+]$  was simulated with a high- $[\text{K}^+]$ -buffered saline solution (mM: 150 KCl, 5  $\text{MgCl}_2$ , 10 HEPES, and 5 KOH, pH 7.2). An ATP-regenerating system consisting of 1 mM  $\text{MgATP}$ , 5 mM creatine phosphate (di-tris salt) and 20 units/ml creatine phosphokinase VI-S (Sigma) was used as substrate for MMT (e.g., [36]). Note that by substrate we mean a substance required for MMT

and, therefore, the term does not include the translocating particle, which we will call heretofore MMT “cargo” after [37].  $\text{Ca}^{2+}$  loading of the NE cisterna as well as part of the MMT substrates were secured with the ATP-regenerating system plus  $1 \mu\text{M}$   $[\text{Ca}^{2+}]$  [15]. Here we refer to this mixture as the Ca+ATP system. Inositol 1,4,5-trisphosphate ( $\text{IP}_3$ , Sigma) and thapsigargin (TSG, LC Laboratories, Woburn, Mass., USA) were applied before or after treatment with the Ca+ATP system. Both substances were applied to the pipette, the bath or both. TSG was used as it has been shown to inhibit the NE  $\text{Ca}^{2+}$  pump in hepatocytes ([38]; note, however, that this does not appear to be the case in the *Xenopus laevis* oocyte preparation, [4]). Since the NE cisterna has side access to all the NPCs in the NE, we used this concept in our experimental design. Thus, applying the  $\text{Ca}^{2+}$ -loading substrate or the  $\text{Ca}^{2+}$ -depleting agent (e.g.,  $\text{IP}_3$ ) to the region outside the pipette tip secured, respectively, the loading or depletion of the NE cisterna under the pipette. This concept is important because it facilitates the experimental design by eliminating  $\text{Ca}^{2+}$  loading of the NE cisterna through the recording pipette. Furthermore, applying the MMT substrate via the pipette made it difficult to record channel activity, as this procedure induces channel plugging (see Fig. 1 in [10]).

### Patch-clamp procedure

Our patch-clamp approach for recording and analyzing NPCC activity is described elsewhere [11, 18, 19]. The data-acquisition system (EPC-7, List Medical, Darmstadt, Germany; TL-125, Axon Instruments, Foster City, Calif., USA) was calibrated with a precision resistor ( $10^9 \Omega$ , Eltec Instruments, Daytona Beach, Fla., USA) and oscilloscope (2225, Tektronix, Beaverton, Ore., USA). As for cardiac myocyte nuclei [18], long-term recordings (1–36 h) were possible with these cancer cell nuclei. Their reversal and resting potentials,  $V_{\text{rev}}$  and  $V_{\text{rest}}$ , were negligible [19]. To counter potential ion accumulation due to electrical field polarization, voltage pulses were delivered to the pipette electrode from 0 mV, the value at which the current reverses direction (i.e.,  $V_{\text{rev}}$ , [19, 35]). Since the outer nuclear membrane of the NE is continuous with the endoplasmic reticulum (ER), a common concern with patch-clamp studies of isolated nuclei is the NE contamination with ER debris (discussed in [18]). A recent study combining patch-clamp with AFM demonstrated such contamination of patch-clamped NE [39]. The fluorescence microscopy experiments detailed below demonstrate that our preparation has functional NPCs and, therefore, that such ER contamination is immaterial to our observations. Channel properties were analyzed with eight-record ensembles of patch current and conductance,  $I_p$  and  $\Gamma_p$ , respectively. Single channel conductance,  $\gamma$ , was measured directly from the current jumps ( $\Delta i$ ) in each current trace and, indirectly, by multi-Gaussian fitting of the cumulative histograms for each trace ensemble (in this case standard deviation is contaminated by background noise). Gigaseals were obtained without applying suction to the lumen of the recording pipette (i.e., only the capillary suction at the pipette tip was sufficient, see [19, 35]). Channel activity was measured with the patch-clamp, nucleus-attached mode, in nuclei devoid of conspicuous ER remains – which could be observed by the  $100\times$  (1.36 NA) oil-immersion objective of our inverted microscope [40]. Attempts to form gigaseals in nuclei with conspicuous ER remains were futile (24 out of 24). The number of nucleus-attached patches studied, 57, resulted from the formation of gigaseals in 68 attempts, or  $\approx 84\%$  (22–24°C). Since  $V_{\text{rev}}$  and  $V_{\text{rest}}$  were negligible, the pipette potential was the negative of the voltage sensed by the NPCs,  $V$ . The 100- $\mu\text{l}$  experimental chamber was perfused at 100  $\mu\text{l}/\text{min}$  to counter evaporation, which would have increased ion concentration and thus shifted  $V_{\text{rev}}$  and  $V_{\text{rest}}$ . Because the number of functional channels,  $N$ , and the open probability of a single channel ( $p_{\text{open}}$ ) could not be precisely determined (i.e., a functional channel may be plugged and thus not detected), the data were reduced to the mean of the average patch conductance:  $\langle \bar{\Gamma}_p(t) \rangle$ . Note that for a system of identical, independent channels,  $\langle \bar{\Gamma}_p \rangle = \gamma N p_{\text{open}}$  [19]. Therefore, if  $N$  and  $\gamma$  do not change, then the relative value of  $\Gamma_p$  ( $\text{Rel}\Gamma_p$ ) equals the

relative value of the open probability for the channel population, ( $\text{Rel}P_{\text{open}} = \text{Rel}Np_{\text{open}}$ ). That is,  $\text{Rel}P_{\text{open}} = \text{Rel}\Gamma_p$ . Values are given as mean  $\pm$ SD.

### Laser-scanning confocal fluorescence microscopy

The NPC sieving and transport properties were studied with laser scanning confocal fluorescence microscopy (MRC-600, Bio-Rad, Hercules, Calif., USA; LSM 410, Carl Zeiss, Oberkochen, Germany). Sieving properties were investigated with  $1 \mu\text{M}$  FITC-labeled dextrans (4–150 kDa, Sigma). Macromolecular entry was studied with 100 nM B-phycoerythrin (240 kDa, Molecular Probes, Eugene, Ore., USA) conjugated to the nuclear localization signal (NLS) of the SV40 large T antigen (Sigma). Macromolecular export was studied with FITC-labeled ribonucleotides (rNTPs, Amersham, Arlington Heights, Ill., USA; Boehringer Mannheim, Mannheim) supplemented with cell lysate. An EGFP plasmid (pEGFP-C1  $\approx 3.1$  MDa, Clontech Labs, Palo Alto, Calif., USA) containing the 72-base-pair SV40 enhancer sequence was used to study the NPC capacity for plasmid import. When used with both the lysate and the ATP-regenerating system, transcription factors bind to pEGFP-C1 and hence “cover” it with their NLSs, thus providing nuclear targeting. The experiments with pEGFP-C1 also allowed the study of these isolated nuclei for transcription and translation. The long phase lag (3–6 h) between the import and expression of the plasmid permitted the discrimination between import and export phenomena of the plasmid. The FITC-rNTPs were applied at  $5 \mu\text{M}$  for 30 min under conditions that support transcription (TnT, Promega, Madison, Wis., USA). The probes are then washed out and the export of RNA containing the FITC-rNTPs is imaged.  $\text{Ca}^{2+}$  loading of the NE cisterna was confirmed by imaging the NE with the membrane-permeant form of fluo-3 (fluo-3/AM, Molecular Probes). Nuclei were incubated for 15 min in 100  $\mu\text{M}$  probe and then washed with control saline [15]. Note that for all fluorescent probes, except FITC-rNTPs and fluo-3/AM, the probes were left in the bath as they did not interfere with the imaging of the effect. A total of 136 nuclei were imaged at room temperature (22–24°C).

## Results

### Sieving and macromolecular transport capacity

Our laser-scanning confocal fluorescence microscopy studies showed that nuclei isolated from cultured Dunning G prostate cancer cells have a sieving capacity similar to that of *Xenopus laevis* oocyte nuclei [15]. As shown in Figure 1A, in the absence of  $\text{Ca}^{2+}$  and other MMT substrates, all the cancer cell nuclei allowed the translocation of FITC-dextrans with  $M_r < 10$  kDa (78 out of 78 nuclei, 3 cell culture flasks). The images in Fig. 1A were taken while the probe was in the bath as it does not interfere with the fluorescence microscopy observation of probe translocation (see Materials and methods). In the presence of MMT substrates, nuclear entry of NLS-conjugated B-phycoerythrin was detected in 100% of the nuclei studied (60 out of 60 nuclei, 3 cell culture flasks). These results, shown in Fig. 1B left panel, were similar to those we reported for adult cardiac myocyte nuclei [18]. The light outside the nucleus was caused by the presence of the probe in the bath left there, as it does not interfere with the interpretation of the results (see Materials and methods). Macromolecular export, aided with MMT substrates, could be observed in all the im-

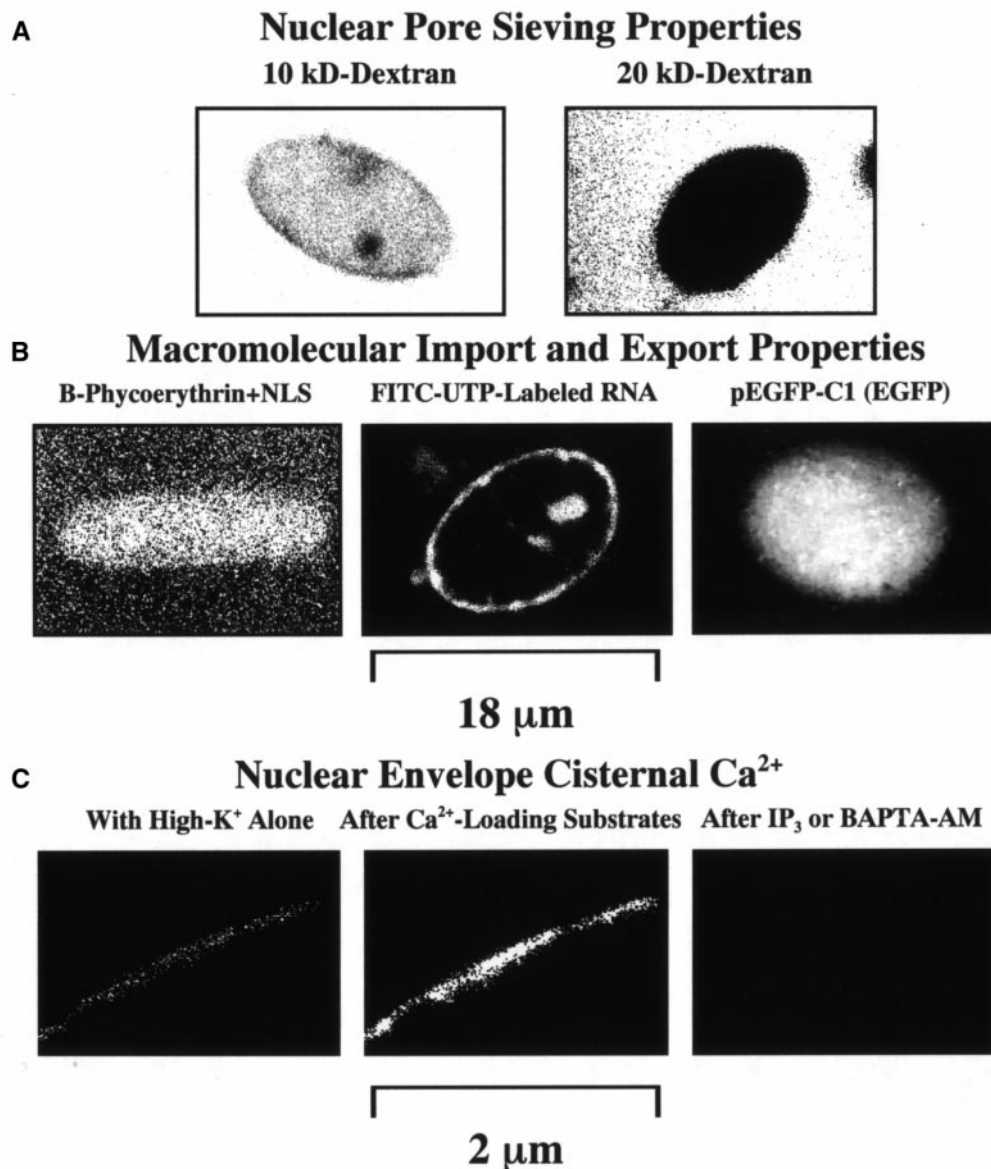


**Fig. 1A–C** Transport properties of nuclei isolated from Dunning G prostate cancer cells. **A** Nuclear pore complex (NPC) functional diameter and passive diffusion limit were estimated with FITC-labeled dextrans. Dextran molecules smaller than 20 kDa translocated to the nucleus. Note that probe washout was not required with confocal microscopy. **B** NPC capacity for macromolecular import was determined with the fluorescent phycobiliprotein B-phycoerythrin (240 kDa) conjugated to the SV40 large T antigen nuclear localization signal (NLS). The image shown was obtained after a 15-min exposure. No washout was required to assess nuclear translocation. The NPC capacity for macromolecular export was estimated by pulse-chase application of FITC-labeled ribonucleotides under conditions that support transcription. The *centered*

*panel* shows an image obtained after washout of the probe mixture and exposure of the nuclei to macromolecular transport substrates. The NPC capacity for simultaneous import, export, transcription and translation was tested with the plasmid for enhanced green fluorescence protein (EGFP, pEGFP-C1 of Mol.Wt.  $\approx$  3.1 MDa). **C** The presence of Ca<sup>2+</sup> in the nuclear envelope (NE) cisterna was determined with the membrane-permeant Ca<sup>2+</sup>-indicator fluo-3/AM. Data in **C** illustrate the common [Ca<sup>2+</sup>]<sub>NE</sub> response in 16 of the 16 nuclei studied. Under control conditions, only a weak signal was detected. However, upon the addition of Ca<sup>2+</sup>-loading substrates, the signal increased. When 1 μM inositol 1,4,5-trisphosphate (IP<sub>3</sub>) or 1 mM BAPTA/AM was added to a control or Ca<sup>2+</sup>-loaded nucleus, no signal was detected

aged nuclei subjected to pulse-chase FITC-rNTPs (46 out of 46 nuclei, 2 flasks). Macromolecular import and export were also observed in all nuclei exposed to the EGFP plasmid, pEGFP-C1 (16 out of 16 nuclei, 2 flasks). Figure 1B center shows the result with the FITC-rNTPs after wash out of the labeled nucleotides (see Materials and methods). Figure 1B right, showing

data obtained with pEGFP-C1, illustrates the capacity of the nuclei for import, export as well as transcription and translation. The plasmid was left in the bath as it did not produce fluorescence. The presence of Ca<sup>2+</sup> in the NE cisterna was determined with the membrane-permeant Ca<sup>2+</sup> indicator fluo-3/AM. Figure 1C illustrates the common [Ca<sup>2+</sup>]<sub>NE</sub> response (16 out of 16 nuclei stud-

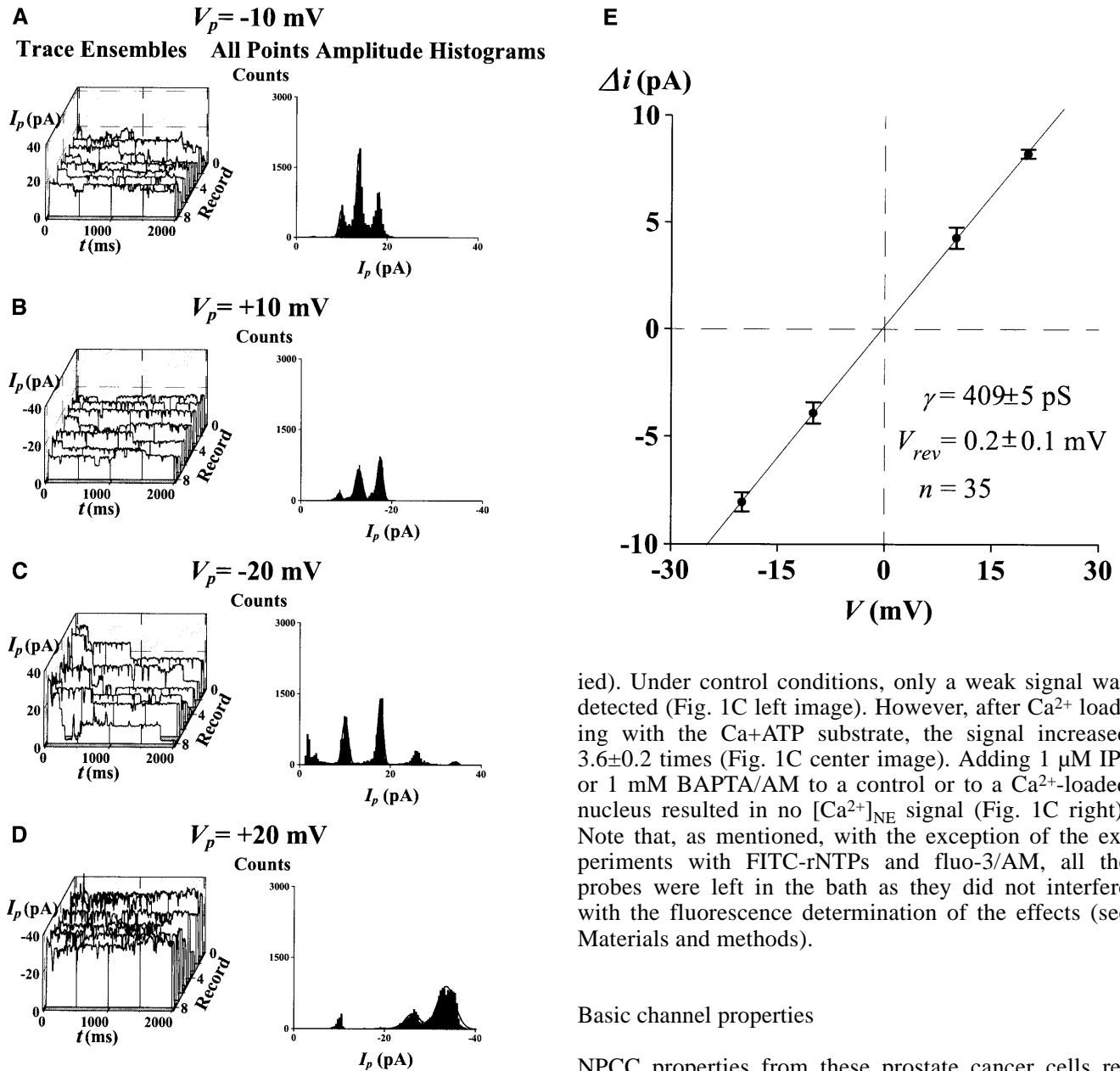


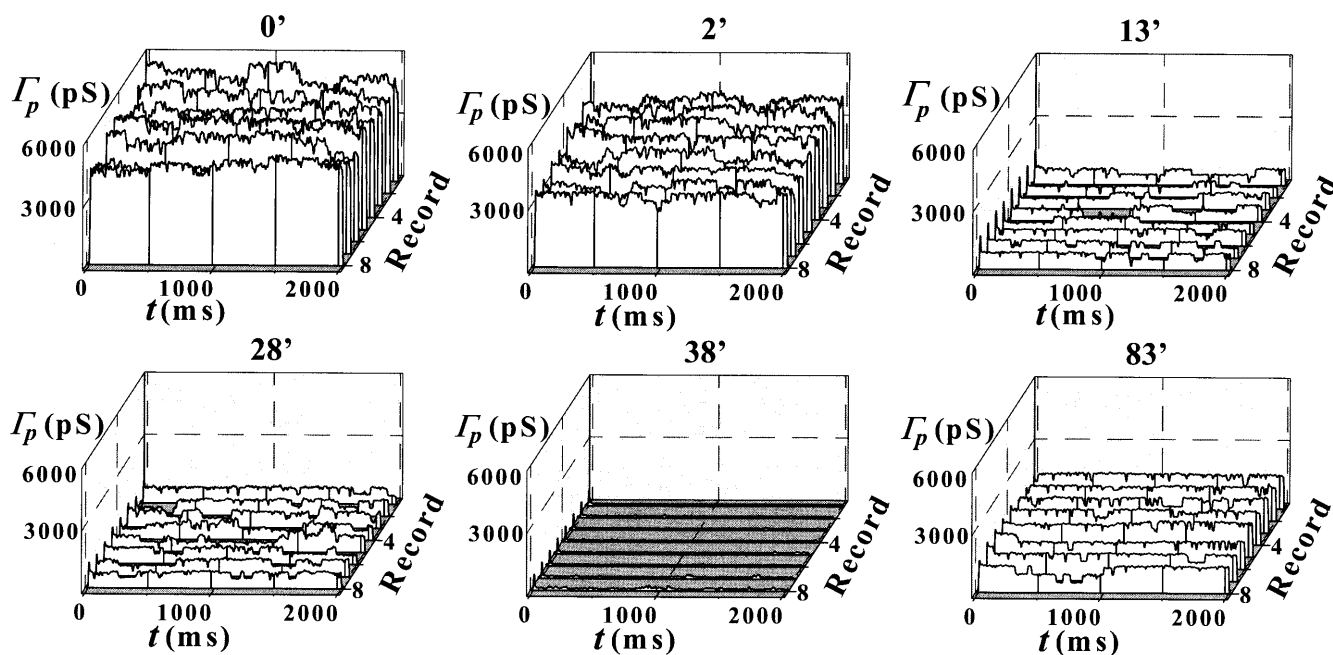
**Fig. 2A–E** Properties of nuclear pore channel (NPC) gating in Dunning G prostate cancer cells. A single experiment, demonstrating the statistical analysis used throughout the patch-clamp investigations. Each individual record of patch current,  $I_p$ , was inspected and single-channel conductance ( $\gamma$ ) calculated. The statistical properties were calculated from the eight-record ensemble. Open–close and close–open transitions were analyzed by direct inspection of each current trace of the ensembles and by analysis of their current histograms **A–D**. From these, open and close probabilities were evaluated. To evaluate the linearity, and thus the voltage dependence, of  $\gamma$  alternating positive and negative pulses were delivered from a holding potential of 0 mV. **A** Graphs corresponding to pulses from 0 to  $-10$  mV (pipette potential). **B–D** Results for pulses from 0 to  $+10$ ,  $-20$ , and  $+20$  mV, respectively. **E** Current–voltage plot obtained from 35 measurements of discrete current transitions,  $\Delta i$

ied). Under control conditions, only a weak signal was detected (Fig. 1C left image). However, after  $\text{Ca}^{2+}$  loading with the  $\text{Ca}+\text{ATP}$  substrate, the signal increased  $3.6 \pm 0.2$  times (Fig. 1C center image). Adding  $1 \mu\text{M}$   $\text{IP}_3$  or  $1 \text{ mM}$  BAPTA/AM to a control or to a  $\text{Ca}^{2+}$ -loaded nucleus resulted in no  $[\text{Ca}^{2+}]_{\text{NE}}$  signal (Fig. 1C right). Note that, as mentioned, with the exception of the experiments with FITC-rNTPs and fluo-3/AM, all the probes were left in the bath as they did not interfere with the fluorescence determination of the effects (see Materials and methods).

#### Basic channel properties

NPCC properties from these prostate cancer cells resemble those previously recorded from adult cardiac myocyte nuclei under similar high-K control conditions (e.g., [18, 19, 35, 41]). Channel activity was detected by measuring the time-dependent ion currents across the NE patch,  $I_p = I_p(t)$ . Figure 2 illustrates the analysis used to characterize the basic properties of channel activity. This analysis is standard in patch-clamp studies and involves single trace and ensemble statistics (see Materials and methods). For the NE patch of Fig. 2, the calculated mean single NPCC conductance  $\gamma$ , measured from 35 discrete quantal jumps ( $\Delta i$ ) in the current records, was  $409 \pm 5$  pS ( $n=35$ ), and the reversal potential,  $V_{rev}$ , was  $0.2 \pm 0.1$  mV ( $n=35$ ). For the 48 control patches investigated, the  $\gamma$  value calculated from 237 discrete quantal jumps in the current records, was  $376 \pm 12$  pS ( $n=237$ ).  $V_{rev}$  in the 57 patches investigated was  $-0.6 \pm 0.1$  mV.

A



B

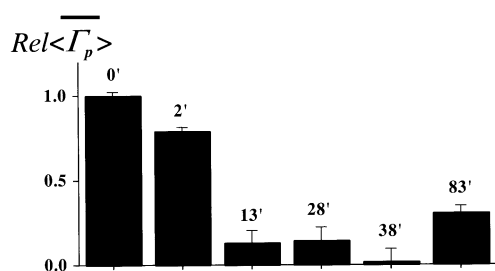


**Fig. 3A–C**  $\text{Ca}^{2+}$  and ATP treatment causes transient plugging of nuclear pores. **A** Record ensembles of patch conductance,  $\Gamma_p(t) = I_p(t)/V$ , obtained at various times of bath application of  $1 \mu\text{M}$   $[\text{Ca}^{2+}]$  plus the Ca+ATP-regenerating system (see Materials and methods). **B** Relative values of the mean of the average traces,  $\langle \Gamma_p(t) \rangle$ , corresponding to the ensembles in **A**. **C** Cumulative histograms for the ensembles in **A**. The calculated single-channel conductance is given for each histogram. Ensembles were generated by applying voltage pulses to the pipette electrode from a holding potential of 0 to a test potential of  $-10 \text{ mV}$

#### Effect of $\text{Ca}^{2+}$ and ATP on channel activity

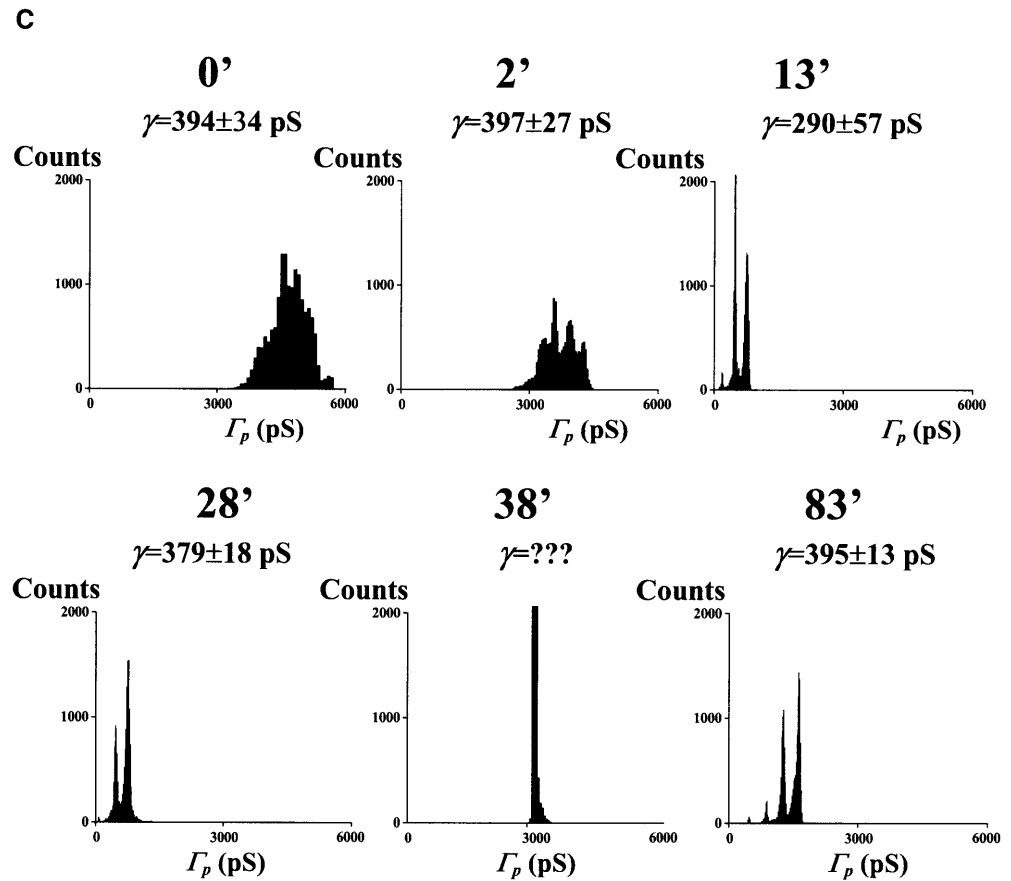
No channel activity was detected 60–90 min following pre-treatment or pipette solution supplementation with  $1 \mu\text{M}$   $[\text{Ca}^{2+}]$  plus the ATP-regenerating system: the Ca+ATP system (12 out of 12 nuclei). This result is identical to our previous observation with adult cardiac myocytes (see Fig. 1 in [10]). Since we agree with the prevalent view that, because of their size, both  $\text{Ca}^{2+}$  and ATP have immediate access to the nuclear interior through unplugged NPCs (see [4]), we utilized this concept to manipulate  $[\text{Ca}^{2+}]_{\text{NE}}$  while recording patch channel activity. Addition of the  $\text{Ca}^{2+}$ -containing, ATP-regenerating

system triggered a transient reduction in both patch and single-channel conductance,  $\Gamma_p$  and  $\gamma$ . This effect appeared within 30 min of chamber perfusion with the Ca+ATP system (19 out of 19 patches). We associated these events with the beginning of MMT because of its slow kinetics and duration of 30–260 min (typical of this mechanism under our experimental conditions) and because of the effects of pre-treatment or pipette loading with the Ca+ATP system. Figure 3 shows highlights from one of these experiments. The graphs in Fig. 3A give the ensembles of patch conductance,  $\Gamma_p(t)$ , at different times of bath perfusion with the Ca+ATP system. The bar graph in Fig. 3B shows the relative change in the mean of  $\langle \Gamma_p(t) \rangle$ ,  $[\text{Rel}\langle \Gamma_p(t) \rangle]$ . Amplitude histograms are given in Fig. 3C. All three characterizations of the events (Fig. 3A–C) demonstrate the period of silence of single-channel activity.

#### Effect of $\text{IP}_3$ and TSG

$\text{IP}_3$ -activated channels were observed in *Xenopus laevis* oocyte nuclei [42, 43]. Pre-incubation of the preparations for 1–5 min with  $1\text{--}5 \mu\text{M}$   $\text{IP}_3$  did not change  $N$ , the number of ion-conducting channels ( $N = 6 \pm 3.6$  in control versus  $N = 5 \pm 3.8$  with  $\text{IP}_3$ , six nuclei each). Note that this number is not necessarily equal to the number of functional channels, as the latter may be greater as it includes plugged NPCs. A similar result was obtained when recordings were made from the pre-treated nuclei with  $\text{IP}_3$ -loaded pipettes ( $N = 6 \pm 3.6$  in control versus  $N = 4 \pm 3.2$  with  $\text{IP}_3$  in both bath and pipette, six nuclei each). We then tested whether the lack of  $\text{IP}_3$  effects are related to reduced  $[\text{Ca}^{2+}]_{\text{NE}}$ . Figures 4 and 5 illustrate the lack of response to  $1\text{--}5 \mu\text{M}$   $\text{IP}_3$  in the absence and

Fig. 3C



presence of the Ca+ATP system (12 out of 12 patches). Like Ca<sup>2+</sup> and IP<sub>3</sub> [15], the Ca<sup>2+</sup>-pump inhibitor TSG depletes the NE cisterna of Ca<sup>2+</sup> [38]. Channel activity was not significantly changed with 1–2 μM TSG, alone or with IP<sub>3</sub> (three out of three patches; not shown). Gating was not directly dependent on ATP, as was shown by the lack of effect of repeated [Ca<sup>2+</sup>]<sub>NE</sub> replenishment after washout of the first [Ca<sup>2+</sup>]<sub>NE</sub>-load treatment. Ca<sup>2+</sup> loading did not affect gating in nuclei with a depleted [Ca<sup>2+</sup>]<sub>NE</sub> by overnight storage at 4°C in a high-[K<sup>+</sup>] storage solution with 5 mM EGTA (three out of three patches; not shown). Application of 1–5 mM BAPTA/AM was inconsequential (four out of four patches; not shown).

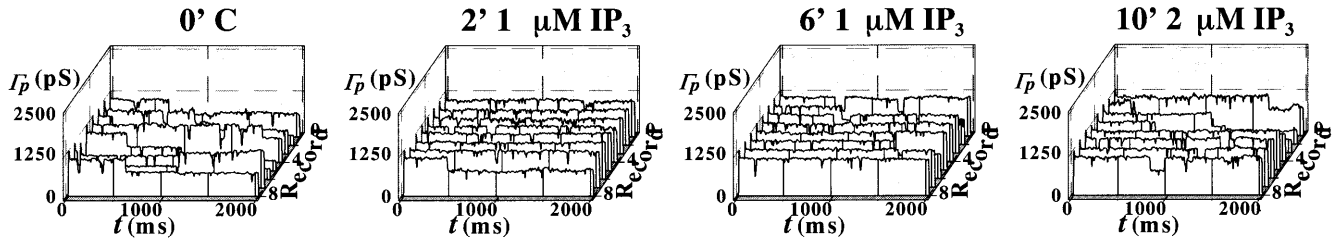
## Discussion

### The NPC ion channel behavior

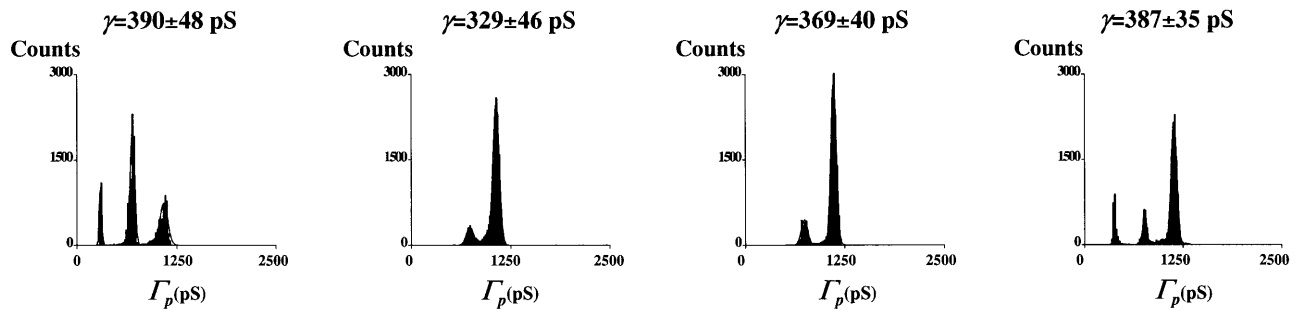
We previously argued with data from MMT-capable cardiomyocyte nuclei that the large- $\gamma$  channel activity (recorded with a pipette attached to the outer membrane of the NE) corresponds to gated ion flow along the NPCC [18]. We showed that the NPC antibody mAb414 (and none of the five other antibodies tested) blocks the large- $\gamma$  channel activity recorded from these nuclei [18]. This demonstration was crucial in identifying the source of

channel activity, because the mAb414 blocks NPC-mediated MMT and localizes in the central region of the NPCC [18, 44, 45]. Our observations with mAb414 were independently confirmed by Prat and Cantiello in 1996 (see [25]). Since in *in situ* conditions the outer NE membrane is connected to the ER, we carried out experiments demonstrating that ER protein-conducting channels are not the source of this channel activity [18]. It was later demonstrated, however, that Ca<sup>2+</sup> triggers the disruption of these two topological regions [34]. It remains to be tested whether intact Dunning G prostate cancer cells display this ER-NE separation. Here we provide evidence that IP<sub>3</sub>-sensitive channels do not contribute to the large- $\gamma$  channel activity recorded from cultured Dunning G prostate cancer cells. We also previously demonstrated that exposure to MMT-supporting conditions, such as reticulocyte lysate, results in the transient silencing of ion channel activity which is directly correlated to the timing of MMT ([18]; see Fig. 1 in [10]). Furthermore, for a preparation such as ours (in which the NPCCs have been demonstrated to be fully functional), the electrical circuit theory dictates that, regardless of the presence of other ion channels (with lower ion conductance and numbers) at either of the two membranes of the NE, the NPCCs (the only pathway connecting the nuclear interior to the cytosol) are a major (if not the major) pathway for an electrical current between the electrode in the recording patch-clamp pi-

A



B



C

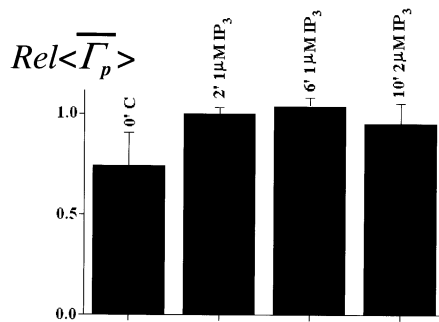


**Fig. 4A–C**  $\text{IP}_3$  does not activate ion channels. **A, B** Trace ensembles and histograms for the different times of bath exposure to 1 and 2  $\mu\text{M}$   $\text{IP}_3$ . **C** Summary of experimental results expressed as a bar graph constructed with the relative mean of patch conductance trace average,  $\langle \overline{\Gamma_p(t)} \rangle$ . Ensembles were generated with 0 to  $-20$  mV pulses applied to the pipette

pette and the electrode in the bath of the perfusion chamber – where the nuclei are placed (reviewed in [12]). Since the number of ion-conducting channels recorded in our preparations is smaller than that seen with electron microscopy (EM, see [18]) it is clear that some of the NPCCs are plugged. That not all NPCCs are plugged may be related to the fact that  $[\text{Ca}^{2+}]_{\text{NE}}$  seems to be high (reviewed in [46]). This characteristic of our preparation facilitates single-channel analysis with current patch-clamp statistical methods and explains why we are successful in achieving gigaseals upon pipette contact with the NE – a preliminary goal and requirement in patch-clamp recording. It is impossible to record more than a gigaohm of seal resistance between the pipette and the NE (i.e., a gigaseal) without some NPCCs being plugged by translocating macromolecules.

#### The macromolecule-conducting ion channel paradigm

We previously introduced our interpretation of the dual nature of the NPC as a transport pathway in what we called the macromolecule-conducting ion channel paradigm [18]. We proposed that, during MMT, the NPCC is plugged by the translocating macromolecules and that when the channel is free of macromolecules it behaves as an ion channel. The time for which the channel is plugged is determined by the size, shape and number of translocating particles, the intrinsic NPC transport capacity, and the availability of transport substrates and components (ATP, GTP, docking site,  $\text{Ca}^{2+}$ , etc.). Thus, in the case of pEGFP-C1 (Mol. Wt.  $\approx 3.1$  MDa), the period of NPCC electrical silence (which we attribute to MMT) lasted 5–10 h. The variability of the silent period may be related to the availability of transport substrates despite the addition of cell lysate. Our recent investigations using patch-clamp and fluorescence of pEGFP-C1 simultaneously support this idea (J.O. Bustamante, E.R.F.M. Michelette, and D.A. Dean). During the tests with nuclear-targeted B-phycoerythrin and FITC-rNTPs we did not add macromolecules to the pipette or bath, except for the few experiments in which we added cell lysate. Thus, it is plausible that, even in those cases where no lysate was added, other molecules (e.g., transcription factors docked at the NPC docking sites) may have contributed to the NPCC plugging following the stimulation of MMT via the increase of  $[\text{Ca}^{2+}]_{\text{NE}}$  caused by adding the Ca+ATP system. It is interesting to note that the TATA-binding protein (TBP), a structural and functional transcription factor, has been reported to transiently modify the single-channel conductance,  $\gamma$ , in the same manner as other macromolecules [22]. TBP also modifies the value of  $\gamma$  (see Fig. 5 in [22]). In addition to increasing the stability of the preparation, TBP modifies the instantaneous

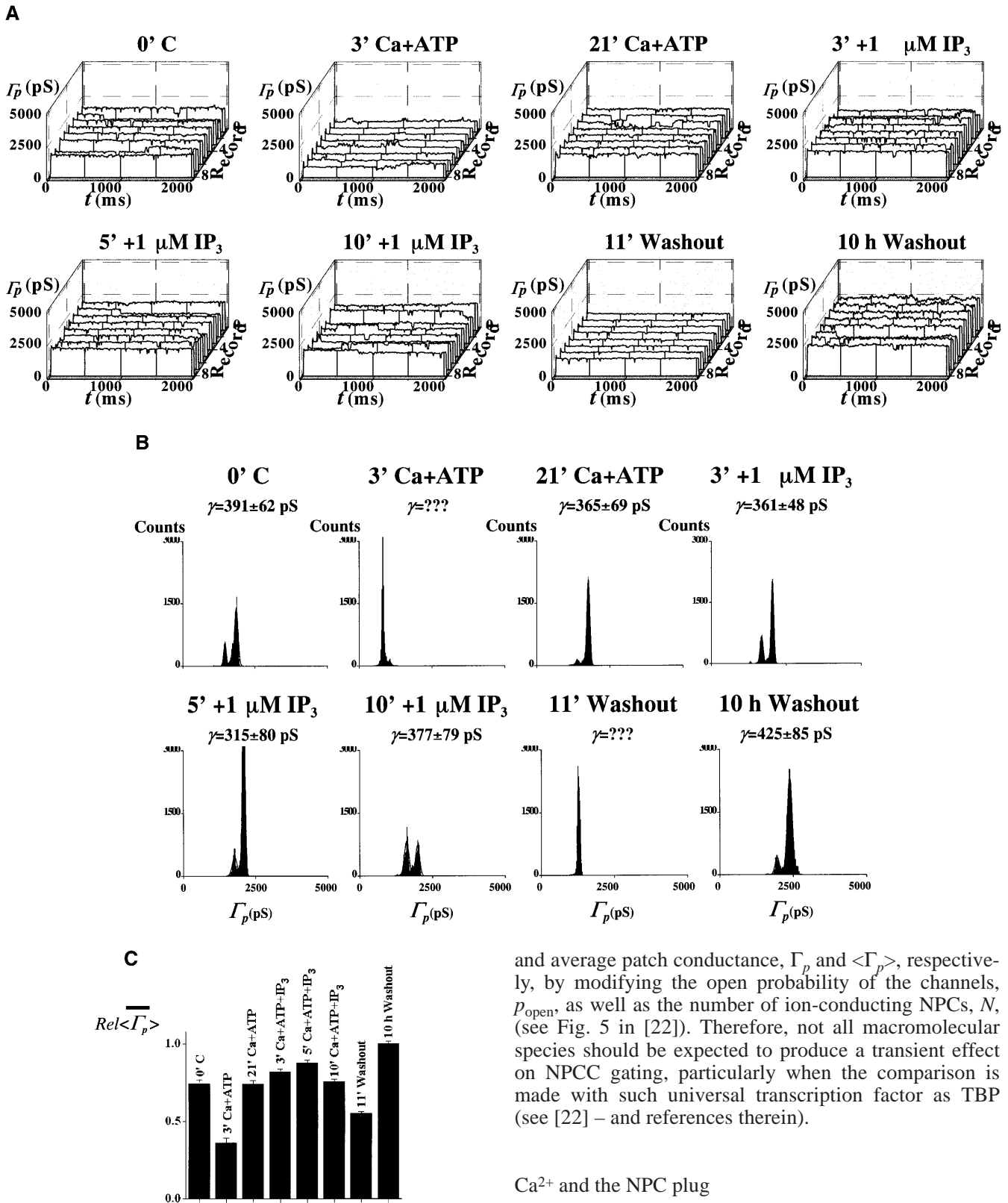


**Fig. 5A–C** IP<sub>3</sub> fails to have a significant effect in Ca<sup>2+</sup>-loaded nuclei. **A, B** Trace ensembles and histograms are given for the different times of bath exposure to IP<sub>3</sub> and Ca<sup>2+</sup>-loading conditions. **C** Bar graph showing changes in relative means of the average conductance,  $\langle \Gamma_p(t) \rangle$ . Pipette voltage pulses were delivered from 0 to –10 mV

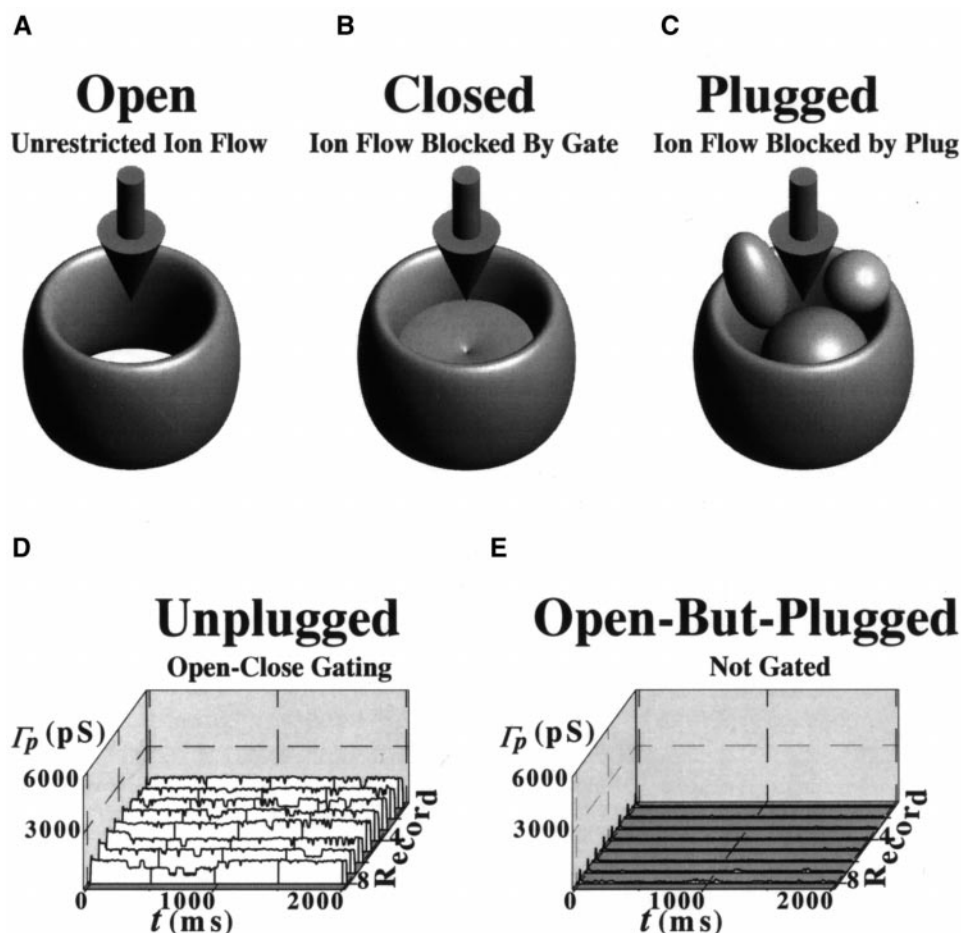


**Fig. 6A–E** NPC channel gating model: the macromolecule-conducting ion channel paradigm. **A–C** NPC models showing three basic states: open (**A**), closed (**B**), and open but plugged (**C**). The downward arrows indicate ion flow. **D, E** The NPC is thought to open and close in a manner similar to that of classic ion channels. The open and close probabilities depend on the conditions to which the NPC is subjected. In an ideally pure binomial system, the open and close probabilities would be equal (i.e., 0.5). This would result in equal probability of seeing open-state and close-state ion current levels (e.g., 1 and 0; note that conductance is current/voltage and that the voltage is constant/clamped). **D** A patch conductance ensemble taken from Fig. 3. The ensemble contains at least three indistinguishable ion-conducting channels. During macromolecular translocation, *MMT*, the NPC channel is plugged and, therefore, the ion current (and conductance) is zero. Thus, an open NPC may be plugged by stimulating *MMT* with, for example,  $\text{Ca}^+$ -ATP and other *MMT* substrates. This, of course, would happen if the preparation were to have macromolecules (e.g., DNA, RNA, transcription factors) available for translocation and/or if the preparation had sufficient substrates for repeated *MMT*. **E** Data from Fig. 3 show the effect of *MMT*. In the paradigm, macromolecule and ion conduction are mutually exclusive. That is, when a macromolecule is being conducted, ions are excluded (and vice versa). Therefore, *MMT* results in reduction of ion flow or current

plug, granule or transporter intrinsic to the NPC, always incorporate central hole (e.g., [47]). However, our interpretation of our results is better represented by recent AFM observations made with a more physiological preparation showing that NPCs have no intrinsic plug [2, 3] and that the putative NPC plug represents a macromolecule caught in transit along the channel. Whether or not  $\text{Ca}^{2+}$  is trapped in the nucleoplasm after  $\text{Ca}^{2+}$  release from the NE cisterna seems to depend on the preparation [48]. Alternative explanations of our observations are plausible. Indeed, Oberleithner [20] demonstrated that, in cultured MDCK kidney cells, NPCs contract seconds after exposure to aldosterone, bradykinin and ionomycin, agents known to trigger a  $\text{Ca}^{2+}$  signal [20]. Our results indicate that repetitive  $\text{Ca}^{2+}$  signals (whether up- or down-regulated) are inconsequential for a pore in an environment devoid of translocating macromolecules. For this reason we subscribe to our original proposal that  $\text{Ca}^{2+}$  only acts indirectly on the NPC.

#### ATP and NPC channel gating

ease of diffusion of monoatomic ions along the NPCC. That is, the plug must have a hole sufficiently large to account for the ion flow always seen in isolated and in situ nuclei. Thus, all NPC structural models developed with high-resolution microscopy and which include a

Rudel et al. [49] showed that ATP and GTP interrupt the activity of the porin-PorB bacterial channel – a structure whose conductance and channel diameter are 1500 pS and 10 nm, respectively [49]. The observations were interpreted by the authors to result from conformational

changes [49]. Although it is possible that the NPCC conformation was affected by our experimental maneuvers, the lack of effect after repeated treatment with the Ca<sup>+</sup>ATP system does not support this alternative. Unfortunately, since Rudel et al. [49] did not try repeated exposures, a direct comparison of these two different channels is not possible. Our study supports the idea that [Ca<sup>2+</sup>]<sub>NE</sub> and ATP, when present in conjunction with all the elements required for MMT, cause a transient reduction of single NPCC ion conductance,  $\gamma$  (and thus NE ion permeability), by promoting transient channel plugging during MMT. Since treatment with the Ca<sup>+</sup>ATP system assists MMT, the treatment would result in increased NE conductance in preparations with plugged NPCs (e.g., [32]). Figure 6 illustrates the macromolecule-conducting ion channel paradigm applied to the NPCC as previously described by us [18].

The NPC channel is indirectly modulated by cytosolic Ca<sup>2+</sup> and ATP

Our results exclude IP<sub>3</sub>-sensitive channels as the source of channel activity because the activity was not enhanced when IP<sub>3</sub> was present in the pipette, the bath or both. Our experimental observations differ from those reported by others reporting enhanced channel activity with IP<sub>3</sub> [42, 43]. We propose that, when combined, Ca<sup>2+</sup> and ATP act indirectly, through the NE cisterna, on NPCC gating. This action results from their combined effects on MMT and, although we found no supporting evidence, they may also act directly on NPCC conformation. While we think that our patch-clamp results are not discrepant with those of Mazzanti's group [32, 33], our interpretation of the data (both ours and theirs) differs in that they propose a direct action of either agent while we argue for an indirect action mediated through MMT. This may be the result of specimen preparation and is a topic that requires further investigation. However, 200-pS rectifying Ca<sup>2+</sup>-activated K<sup>+</sup> channels were reported as present in NE isolated from single pancreatic acinar cells [50]. Therefore, the existence of these channels in other preparations cannot be excluded. We subscribe to the suggestion made by others that a plausible candidate for this mechanism is the NPC transmembrane glycoprotein gp210 ([4, 14, 15, 51] – reviewed in [1]). This glycoprotein contains an EF-hand (helix-loop-helix) Ca<sup>2+</sup>-binding domain facing the NE cisterna.

**Acknowledgements** Supported by grants from the Medical Research Council (MRC) of Canada and the Fundação de Apoio à Pesquisa do Estado de São Paulo (FAPESP) to J.O.B., and from the National Institutes of Health (NIH) to J.P.G., D.A.D. and T.J.McD. We thank Dr. Frederick J. Sigworth (Yale University School of Medicine) for comments. <http://www.geocities.com/TheTropics/6066/index.html>.

## References

- Panté N, Aebi U (1996) Molecular dissection of the nuclear pore complex. *Crit Rev Biochem Mol Biol* 31:153–199
- Stoffler D, Goldie KN, Feja B, Aebi U (1999) Calcium-mediated structural changes of native nuclear pore complexes monitored by time-lapse atomic force microscopy. *J Mol Biol* 287:741–752
- Stoffler D, Fahrenkrog B, Aebi U (1999) The nuclear pore complex: from molecular architecture to functional dynamics. *Curr Opin Cell Biol* 11:391–401
- Pérez-Terzic C, Pyle J, Jaconi M, Stehno-Bittel L, Clapham DE (1996) Conformational states of the nuclear pore complex induced by depletion of nuclear Ca<sup>2+</sup> stores. *Science* 273:1875–1877
- Pérez-Terzic C, Gacy AM, Bortolon R, Dzeja PP, Puceat M, Jaconi M, Prendergast FG, Terzic A (1999) Structural plasticity of the cardiac nuclear pore complex in response to regulators of nuclear transport. *Circ Res* 11:1292–1301
- Wang H, Clapham DE (1999) Conformational changes of the in situ nuclear pore complex. *Biophys J* 77:241–247
- Lee MA, Dunn RC, Clapham DE, Stehno-Bittel L (1998) Calcium regulation of nuclear pore permeability. *Cell Calcium* 23:91–101
- Badminton MN, Kendall JM, Salanewby G, Campbell AK (1995) Nucleoplasmin-targeted aequorin provides evidence for a nuclear calcium barrier. *Exp Cell Res* 216:236–243
- Al-Mohanna FA, Caddy KWT, Bolsover SR (1994) The nucleus is insulated from large cytosolic calcium ion changes. *Nature* 367:745–750
- Bustamante JO (1994) Nuclear electrophysiology. *J Membr Biol* 138:105–112
- Bustamante JO, Liepins A, Hanover JA (1994) Nuclear pore complex ion channels. *Mol Membr Biol* 11:1414–150
- Bustamante JO, Varanda WA (1998) Patch-clamp detection of macromolecular translocation along nuclear pores. *Braz J Med Biol Res* 31:333–354
- Stehno-Bittel L, Perez-Terzic C, Luckhoff A, Clapham DE (1996) Nuclear ion channels and regulation of the nuclear pore. *Soc Gen Physiol Ser* 51:195–207
- Greber UF, Gerace L (1995) Depletion of calcium from the lumen of endoplasmic reticulum reversibly inhibits passive diffusion and signal-mediated transport into the nucleus. *J Cell Biol* 128:5–14
- Stehno-Bittel L, Pérez-Terzic C, Clapham DE (1995) Diffusion across the nuclear envelope inhibited by depletion of the nuclear Ca<sup>2+</sup> store. *Science* 270:1835–1838
- Tonini RF, Grohovaz CA, Laporta M, Mazzanti M (1999) Gating mechanism of the nuclear pore complex channel in isolated neonatal and adult mouse liver nuclei. *FASEB J* 13:1395–1403
- Keminer O, Peters R (1999) Permeability of single nuclear pores. *Biophys J* 77:217–228
- Bustamante JO, Hanover JA, Liepins A (1995) The nuclear pore ion channel activity. *J Membr Biol* 146:239–251
- Bustamante JO (1992) Nuclear ion channels in cardiac myocytes. *Pflügers Arch* 421:473–485
- Oberleithner H (1999) Aldosterone and nuclear signaling in kidney. *Steroids* 64:42–50
- Rakowska A, Danker T, Schneider SW, Oberleithner H (1998) ATP-induced shape change of nuclear pores visualized with the atomic force microscope. *J Membr Biol* 163:129–136
- Bustamante JO, Liepins A, Prendergast RA, Hanover JA, Oberleithner H (1995) Patch-clamp and atomic force microscopy demonstrate TATA-binding protein (TBP) interactions with the nuclear pore. *J Membr Biol* 146:263–272
- Bustamante JO, Oberleithner H, Hanover JA, Liepins A (1995c) Patch-clamp detection of transcription factor translocation across nuclear pores. *J Membr Biol* 146:253–261
- Bustamante JO, Prendergast R, Hanover JA, Oberleithner H, Liepins A (1995) Macromolecular translocation reduces ion flow along nuclear pores: relevance to measuring transcriptional control mechanisms. *J Gen Physiol* 105:25–26a

25. Prat AG, Cantiello H (1996) Nuclear ion channel activity is regulated by actin filaments. *Am J Physiol* 270:C1532–C1543
26. Henry JP, Chich JF, Goldschmidt D, Thieffry M (1989) Blockage of a mitochondrial cationic channel by a mitochondrial addressing peptide. *CR Acad Sci III* 309:87–92
27. Henry JP, Juin P, Vallette F, Thieffry M (1996) Characterization and function of the mitochondrial outer membrane peptide-sensitive channel. *J Bioenerg Biomembr* 28:101–108
28. Liu MY, Colombini M (1992) A soluble mitochondrial protein increases the voltage dependence of the mitochondrial channel, VDAC. *J Bioenerg Biomembr* 24:41–46
29. Liu MY, Torgrimson A, Colombini M (1994) Characterization and partial purification of the VDAC-channel-modulating protein from calf liver mitochondria. *Biochim Biophys Acta* 1185:203–212
30. Colombini M, Blachly-Dyson E, Forte M (1996) VDAC, a channel in the outer mitochondrial membrane. *Ion Channels* 4:169–202
31. Lohret TA, Kinnally KW (1995) Targeting peptides transiently block a mitochondrial channel. *J Biol Chem* 270:15950–15953
32. Mazzanti M, Innocenti B, Rigattelli M (1994) ATP-dependent ionic permeability on nuclear envelope in situ nuclei of *Xenopus* oocytes. *FASEB J* 8:231–236
33. Assandri R, Bertaso F, Mazzanti M (1995) Modulation of nuclear ion conductance by Ca and ATP. *Biophys J* 68:A20
34. Subramanian K, Meyer T (1997) Calcium-induced restructuring of nuclear envelope and endoplasmic reticulum calcium stores. *Cell* 89:963–971
35. Bustamante JO (1993) Restricted ion flow at the nuclear envelope of cardiac myocytes. *Biophys J* 64:1735–1749
36. Adam SA, Sterne-Marr R, Gerace L (1992) Nuclear protein import using digitonin-permeabilized cells. *Methods Enzymol* 219:97–110
37. Nigg EA (1997) Nucleocytoplasmic transport: signals, mechanisms and regulation. *Nature* 386:779–787
38. Lanini L, Bachs O, Carafoli E (1992) The calcium pump of the liver nuclear membrane is identical to that of endoplasmic reticulum. *J Biol Chem* 267:11548–11552
39. Danker T, Mazzanti M, Tonini R, Rakowska A, Oberleithner H (1997) Using atomic force microscopy to investigate patch-clamped nuclear membrane. *Cell Biol Int* 21:747–757
40. Bustamante JO (1991) An inexpensive inverted microscope for patch-clamp and other electrophysiological studies at the cellular level. *Pflügers Arch* 418:608–610
41. Bustamante JO (1994) Open states of nuclear envelope ion channels in cardiac myocytes. *J Membr Biol* 138:77–89
42. Mak DOD, Foskett JK (1994) Single-channel inositol 1,4,5-trisphosphate receptor currents revealed by patch-clamp of isolated *Xenopus* oocyte nuclei. *J Biol Chem* 269:29375–29378
43. Stehno-Bittel L, Luckhoff A, Clapham DE (1995) Calcium release from the nucleus by  $InsP_3$  receptor channels. *Neuron* 14:163–167
44. Akey CW, Goldfarb DS (1989) Protein import through the nuclear pore complex is a multi-step process. *J Cell Biol* 109:971–982
45. Clever J, Yamada M, Kasamatsu H (1991) Import of simian virus 40 virions through nuclear pore complexes. *Proc Natl Acad Sci USA* 88:7333–7337
46. Petersen OH, Gerasimenko OV, Gerasimenko JV, Mogami H, Tepikin AV (1998) The calcium store in the nuclear envelope. *Cell Calcium* 23:87–90
47. Kiseleva E, Goldberg MW, Allen TD, Akey CW (1998) Active nuclear pore complexes in *Chironomus*: visualization of transporter configurations related to mRNP export. *J Cell Sci* 111:223–236
48. Badminton MN, Kendall JM, Rembold CM, Campbell AK (1998) Current evidence suggests independent regulation of nuclear calcium. *Cell Calcium* 23:79–86
49. Rudel T, Schmid A, Benz R, Kolb H-A, Lang F, Meyer TF (1966) Modulation of *Neisseria* porin (PorB) by cytosolic ATP-GTP of target cells: parallels between pathogen accommodation and mitochondrial endosymbiosis. *Cell* 85:391–402
50. Maruyama Y, Shimada H, Taniguchi J (1995)  $Ca^{2+}$ -activated  $K^+$ -channels in the nuclear envelope isolated from single pancreatic acinar cells. *Pflügers Arch* 430:148–150
51. Greber UF, Gerace L (1992) Nuclear protein import is inhibited by an antibody to a luminal epitope of a nuclear pore complex glycoprotein. *J Cell Biol* 116:15–30